Optica Applicata, Vol. XXXI, No. 1, 2001

Test stands for measuring the average diameter of the fuel aerosol drops by diffraction method

TADEUSZ A. OPARA

Institute of Aviation Technology, Military University of Technology, ul. Kaliskiego 2, 00–908 Warszawa, Poland.

Measuring stands enabling practical implementation the diffraction method for measuring the drop sizes of the fuel aerosol stream are presented. The construction of diffractometer is described in which the recording of the light intensity distribution is made by scanning the image plane with a detecting system adjusted to the specificity of the image. A stand for measuring the average drop diameter in aerosols produced by fuel injectors of airplane turbine engines are presented and exemples of the examination results are shown.

1. Introduction

The particle sizing is nowadays one of the most intensively developing fields of metrology. This follows from the still increasing demand for information about the microstructure of media being the subject of interest in many fields of science, technique and technology (physics of atmosphere, astrophysics, physics of ocean, geology, physical chemistry, biology, botanics, pharmacy, thermodynamics of burning processes, agriculture, metallurgy, as well as textile, food, chemical, cosmetic industries, and the like). The measurements carried out are both of fundamental significance (examination of: flow and decay of liquid stream, the dissolution processes, sorption, flocculation, aggregation, cavitation, coalescence, coagulation processes and the like) and have the utility aspects (monitoring the atmosphere state, quality control, diagnostic of combustion engines and the like).

Recognition of the microstructure of dispersive media is a multifield problem. On the one hand, there exist some autonomic problems dealing with the functioning of research methods applied (physical model of the exploited phenomena, metrological model, measuring device), on the other hand, we have the results the interpretation of which is the final aim of experimental works carried out in the definite fields of science and technology.

The optical methods for particle sizing in dispersive systems are being developed in the most intensive way. In the scientific and technological literature related to this problem a disproportion can be noticed consisting in decisive domination of the number of theoretical elaborations devoted to interaction of light with the

dispersive medium over the works describing the detailed questions connecetd with the apparatus and experimental data processing.

In papers [1]–[6], construction of the devices used for recording the intensity distribution of light scattered under a small angle approximation has been presented. These devices are designed to examine liquid solutions placed in special vessels. Conducting similar measurements in aerosol stream is much more difficult. This follows from both the dynamic character of the effect occurring in the pulverization cone (primary and secondary decays, drop evaporation) and the necessity of protecting the optical elements from contact with liquid drops diffusing in the region of light wave propagation.

The difficulties connected with the recording of light distribution diffracted by the aerosol drops intensify in the case of examination of short duration phenomena (such as injection of fuel to the combustion chamber of piston engines self-ignition acting [7]).

In papers [8]–[11], theoretical principles of the diffraction method for aerosol drop sizing are described. The algorithms rendering it possible to calculate the average diameter D_ρ of the drops in the stream of pulverization spectrum $\rho(D)$ under different variants of diffraction image recording have been presented. For practical needs of these measurements a few examination stands have been designed and adapted to the specificity of dispersive agent producing the fuel aerosol. The common elements of all the designed stands are:

- a system of plane monochromatic wave generation,
- a diffusor producing the aerosol stream,
- an objective realizing the Fourier transforming,
- a system recording the diffraction image.

The possibilities of obtaining satisfactory results of measurement are to the highest degree dependent on the way the diffraction images are recorded.

2. Stand for measuring the light intensity in diffraction images

When measuring directly the scattered light intensity $I(r)$ two basic techniques are used: scanning of the chosen area with the aid of a single photodetector or with a mosaic system composed of a large number of photodetectors. The standard versions of these devices cannot always be used especially in the case of high values of light flux $\Phi = IA$, (A – surface area). In many cases there appears the necessity of designing the detecting systems adjusted to the specificity of the effects under examination.

The essence of the diffraction measuring methods is the analysis of images appearing as a result of plane monochromatic wave diffraction in the aerosol stream. The carrier of information about the drop sizes in the fuel stream under examination is the light intensity distribution $I_F(r)$ in the diffraction surrounding $I_0(r)$ appearing around the focus image $I_0(r)$, (Fig. 1). The light intensity in the focus region $I_0(r)$ is usually several times higher than the maximum value of the light intensity $I_{F\max}$ of the diffraction beam.

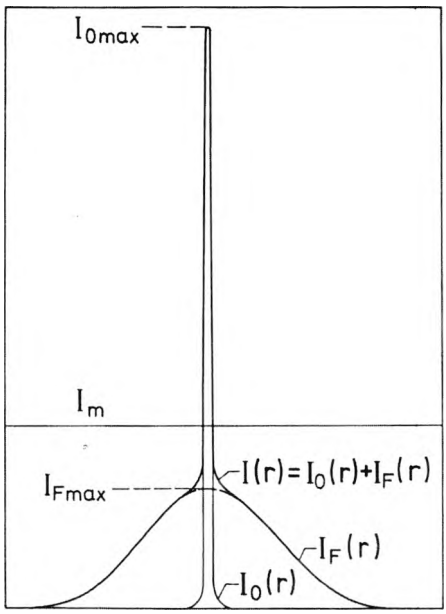

Fig. 1. Light intensity distribution $I(r)$ after the plane parallel light wave has been passed through the aerosol stream.

When using the helium-neon lasers as sources of monochromatic light the radiation intensity in the focus can reach the values as high as $I_0 = 1-10$ kW/m^2 which are too high for the majority of mosaic detector systems to be applied. Besides, for such high differentiation of the emission flux $\Phi(r)$ on the surface of the mosaic photodetector a diffusion of light occurs which leads to a significant broadening of the image focus and to deformation of the useful part of the distribution $I_F(r)$. This effect can be eliminated by scanning the diffraction image with a single photodetector of limited input aperture. This, however, requires designing of a detector system satisfying two mutually contradictory requirements following from the specificity of the examined light intensity distribution $I(r) = I_F(r)+I_0(r)$, which results in the high disproportion between the maximum values of both components $I_{F\max} \ll I_{0\max}$ (Fig. 1).

The metrological problem described is essentially simplified by applying a suitable mask which allows the focus image to be screened. The masking is, however, an operation which causes loss of a part of information about the intensity distribution $I(r)|_{r\to 0}$, the latter being indispensable to determine accurately the distribution $I_F(r)$ as a result of Fraunhofer diffraction by the drops of the aerosol examined.

In order to verify the variants of the measuring method worked out a sensitive scanner of diffraction images has been designed, the most important element of which is the detection system [12], [13]. The concept of high intensity distribution $I(r)$ for the value $r \to 0$ consists in applying a gauge which would not suffer from destruction during short exposure in the region of plane wave focus. For this purpose, such a photodetector should be chosen which preserved its parameters

even when exposed to the extreme value of light intensity $I_{0\max}$ and which, on the other hand, would provide an accurate measurement of the much weaker "diffraction" part of the distribution $I_{F\max}(r)$.

The most important advantage of such a way of measuring is the possibility of applying a difference technique to determine the component $I_F(r) = I(r) - I_0(r)$. Before the proper measurements are made the image of the focus $I_0(r)$ is recorded together with the background which appears around the focus as a result of scattering effect and diffraction by all kinds of pollutants occurring on the surface of optical elements and in the whole space within which the light wave propagates. The knowledge of the distribution $I_0(r)$ allows the light intensity value $I_{F\max}$ to be essentially corrected. This correction has a principal significance for the diffraction method applied due to its great influence on the systematic error which occurs during the analysis of the experimental data.

2.1. Concept of the measuring stand

In Figure 2, an optical scheme of the detecting system is shown. The light beam after having passed through the interference filter (1) hits the ground glass (2) behind which a diaphragm (3) with an aperture of diameter D_a is located. The objective (4) produces a magnified real image of the input diaphragm overlapping the active area of the photodetector of diameter D_{ph}. The decrease of the light wave intensity is inversely proportional to the square of the image magnification $p = D_{ph}/D_a$

$$\frac{I_{ph}}{I_a} = \frac{1}{p^2} \tag{1}$$

where: I_{ph} — light wave intensity on the photodetector surface and I_a — light wave intensity at the diaphragm aperture.

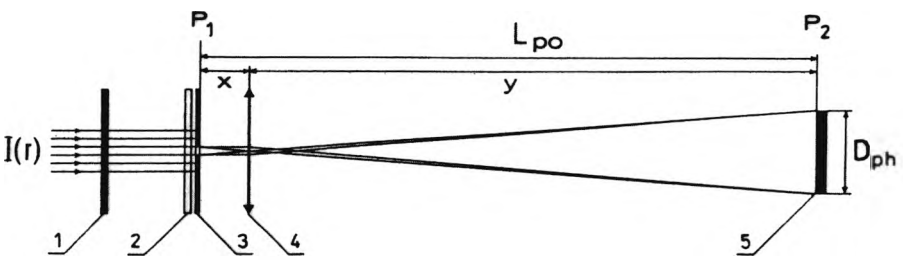

Fig. 2. Scheme of the detection system (1 — interference filter, 2 — ground glass, 3 — entrance diaphragm of aperture diameter D_a, 4 — objective, 5 — photodetector).

The resolving power is being increased during the process of scanning by diminishing the diameter of the entrance diaphragm D_a. For the value $D_a \leqslant 0.05$ mm the application of ground glass (2) and the objective (4) is no more justified since the diaphragm aperture starts to play part of a diffraction "lens".

In the photodetector plane a characteristic image $I_{ph}(r)$ appears in the form of Airy rings. Between the maximum light wave intensity $I_{ph\max}$ at the central point of

the photodetector and the intensity I_a in the entrance diaphragm space the following relation holds:

$$\frac{I_{ph\max}}{I_a} = \left(\frac{\pi D_a^2}{4\lambda l}\right)^2 \tag{2}$$

where: λ — light wavelength, l — distance between the entrance diaphragm and photodetector.

This solution offers the advantage of accurate determination of the proportion m between the light flux Φ_a in the diaphragm space (pinhole) and the flux Φ_{ph} on the active surface of the photodetector

$$m = \frac{\Phi_{ph}}{\Phi_a} = \frac{\int_0^{2\pi}\int_0^{D/2} rI_{ph}(r)drd\varphi}{\int_0^{2\pi}\int_0^{\infty} rI_{ph}(r)drd\varphi}. \tag{3}$$

In the region of the image plane limited by the first dark fringe of diameter [14]–[16]

$$D_0 = 2l\tan\Theta_0 \tag{4}$$

where: $\Theta_0 = \arcsin\left(\frac{1.22\lambda}{D_a}\right)$,

this indicator takes the value of $m = 83.3\%$.

The geometry of the optical system can be conveniently defined by dimensionless parameter

$$z_{uo} = \frac{\pi D_a^2}{\lambda l}. \tag{5}$$

In Table 1 the values of z_{uo} for the indices m changing within the range 10–80% are presented.

In the case of applying the detectors functioning correctly only for small differentiation of the light intensity the parameter z_{uo} can be determined taking advantage of the data in Tab. 2, in which the values m and z_{u0} are listed together with the contrast coefficient

Table 1. Dependence of dimensionless parameters of the optical system z_{uo} on the value of m index.

m [%]	z_{uo}	m [%]	z_{uo}
10	0.649	50	1.680
20	0.946	60	1.949
30	1.196	70	2.280
40	1.436	80	2.817

Table 2. Dependence of m index and parameter z_{u0} on the contrast coefficient k.

k	m [%]	z_{u0}	k	m [%]	z_{u0}
0.99	4.0	0.200	0.94	23.9	0.496
0.98	8.0	0.284	0.93	27.8	0.537
0.97	12.0	0.349	0.92	31.8	0.576
0.96	15.9	0.403	0.91	35.7	0.612
0.95	19.9	0.452	0.90	39.7	0.646

$$k = \frac{I_{ph}\left(\frac{1}{2}D_{ph}\right)}{I_{ph}(0)} = \frac{I_{ph\min}}{I_{ph\max}}. \tag{6}$$

The knowledge of parameter z_{u0} is needed in order to determine the distance L_{p0} between the entrance diaphragm and the photodetector surface (Fig. 2).

The basic function of both variants of the optical system (with objective and without objective) is to create the possibility of controlling the diminishing of the light wave intensity $I(r)$ within the range $I_{ph\max}/I_a = 10^{-1} - 10^{-6}$ and to provide a possibly great part of the input flux Φ to the active area of the photodetector, so that $\Phi_{ph}/\Phi_a = 0.5 - 0.9$.

In order to determine exactly the "diffraction" part of the light intensity distribution $I_F(r)$ it suffices to know the distribution $I(r)$ and $I_0(r)$ within the range not exceeding the value $I_m = 1.5 I_{F\max}$. The intensity I_m defines the top value in the entire distribution $I(r) = I_0(r) + I_F(r)$ containing the information essential for the diffraction method applied (Fig. 1).

The light wave intensity $I(r)$ should be diminished to such a degree that the value I_m be brought to the end of the linear range of the photodetector. It should be chosen in such a way that the maximal admissible light intensity causing no changes of its property I_d were significantly greater than the value $I_{l\max}$ limiting the range of proportional changes. In this way the values $I(r) > I_m$ which are not essential in the implementation of the measuring methods are shifted outside the linear range of photodetector.

2.2. Construction of optical system

Figure 3 illustrates the construction of both the optical and detection systems. After having passed the interference filter (1) the light beam falls on the ground glass behind which the entrance diaphragm (2) is located. The ground glass and the diaphragm are installed in a regulation tube (6) which renders it possible to change their position with respect to the focal plane of the objective in the range $\Delta x =$ 10 mm.

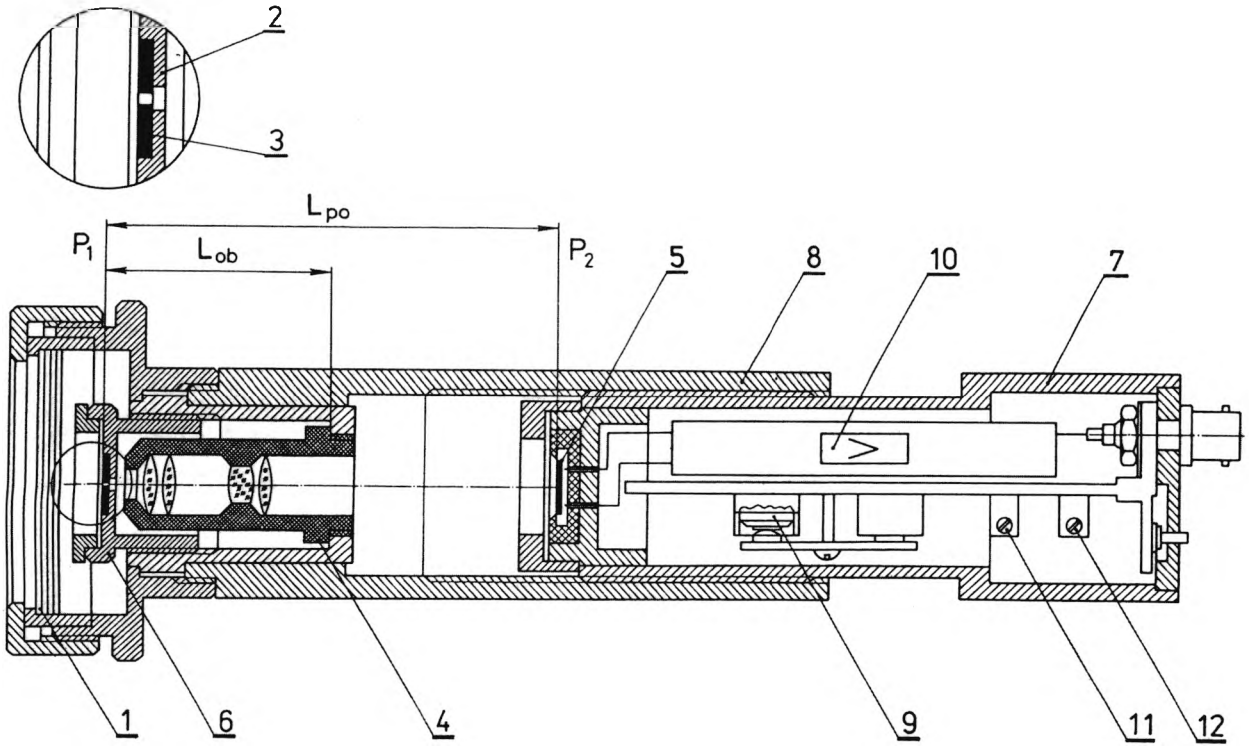

Fig. 3. System for measuring light intensity in the diffraction image (1 — interference filter, 2 — ground glass, 3 — entrance diaphragm, 4 — microscope objective, 5 — active area of the photodetector, 6 — tube controlling the distance between the entrance diaphragm and the objective, 7 — tube to regulate the distance between the objective and the photodetector, 8 — installation tube, 9 — well of cells supplying the amplifier, 10 — amplifier together with the signal transducing system, 11 — screw for compensation of the photocurrent coming from the background, 12 — screw for regulation of the limitation level of the output signal).

The detection and signal transducing systems fill the inside of the sleeve (7) allowing displacement of the photodetector within the range $\Delta y = 55$ mm. The sleeves (6) and (7) allow us to control the distance $L_{po} = x + y$ (Fig. 2) from its minimal value $L_{\min} = 65$ mm to its maximal value $L_{\max} = 130$ mm. The magnification of the entrance diaphragm image $p = y/x$ changes by the factor of 2 in the extreme positions of sleeve (7), *i.e.*, $p_{\max}/p_{\min} = 2$. Applying the entrance diaphragms of aperture diameters creating a dimension series $D_a = 2.00, 1.00, 0.50, 0.25, 0.10$ mm, an arbitrary magnification of their images can be attained within the range $p = 2-100$. The magnitude of the image on the surface of the photodetector as well as the distances x and y will be changed during the adjusting regulation.

The scanning of the diffractive image $I(r)$ is carried out properly when the image surface P_F of the objective realizing the Fourier transformation of the plane monochromatic wave propagating through the aerosol stream examined covers of object P_1 of the optical system presented in Figs. 2 and 3. Thus, each change in position of the controlling sleeve (6), in which the ground glass and diaphragm are installed must be compensated by a suitable shift of the whole system in the opposite direction. By applying two additional elements the necessity of adjusting the distances x and y can be eliminated while assuring simultaneously a constant position of the object plane P_1 and uniform illumination of the active area of the photodetector P_2. These elements are a modified sleeve (6) and additional distance sleeve which assure geometrical conditions enabling use of the parafocallity of the objectives applied (the series Ob 54, Ob 103c, Ob 203c, Ob 404 and Ob 1003P PZO).

The modified sleeve (6), $L_{ob} = 45$ mm, and the distance tube (lengthening the installation tube by 135 mm) assure that the dimensions of the measuring system shown in Fig. 3 meet the standards of Polish Optical Works. Thus, a reduced version of optical microscope (without eyepiece) is created the magnification of which is equal to transversal magnification of the objective β_{ob}.

2.3. Photodetector and the signal transducing system

In order to detect the light radiation a silicon photoelement of BPYP 07 A type (ITE CEMI), the light sensitive layer of which is of area $A_{ph} = 1.00$ cm^2, has a diameter $D_{ph} = 12.732$ mm. For the light of wavelength $\lambda_0 = 0.63$ μm the relative sensitivity of the BPYP 07A photoelement has the value close to the maximal since $S_{\lambda 0} = 0.9$ (Fig. 4).

The BPYP 07A photoelement loaded with the resistance of a few ohms generates the photoelectric current I_p proportional to the light radiation intensity E_v up to the maximal admissible value E_e. For metrological reasons it is advantageous to transform the current signal into voltage signal. The conversion of the photoelectric current I_p generated by the BPYP 07A photoelement has been performed in the systems of both thermally compensated difference amplifier and operational measurement amplifier. By applying the LM 725 system characterized by very small value of polarization current and high voltage amplification in the open loop of feedback the conditions for correct conversion were attained.

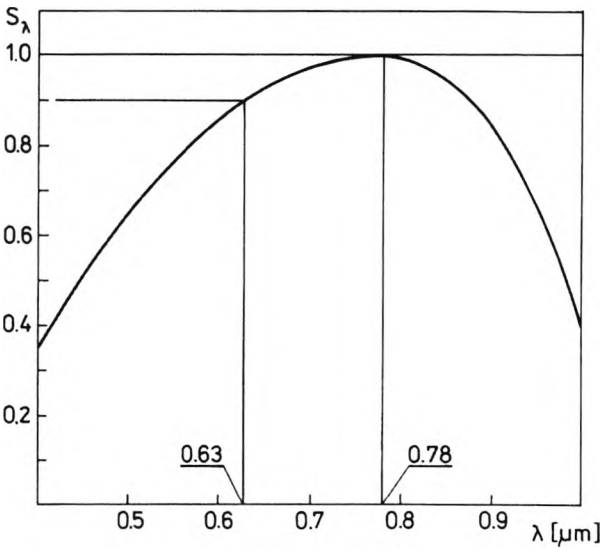

Fig. 4. Spectral dependence of the relative sensitivity $S(\lambda)$ of the BPYP 07A photocell.

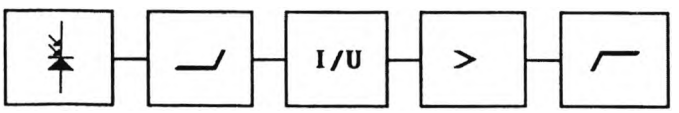

Fig. 5. Block scheme of the system transducing the photoelectric current I_p into the voltage signal U_v.

In Figure 5, a block scheme of the photoelectric current transducing system is shown for the current generated by the BPYP 07A photoelement.

A monochromatic light flux $\Phi(\lambda_0)$ generated by the helium-neon laser as well as the flux $\Phi'(\lambda)$ of the light coming from the surroundings and transmitted by the interference filter SIF 633 ($\lambda_{max} = 0.633$ μm, $T(\lambda_{max}) = 95\%$, $\Delta\lambda_{0.5} = 0.0095$ μm) reach the photoelement surface via the optical system (Figs. 2, 3). The light flux of the background is small $\Phi'(\lambda) \ll \Phi(\lambda_0)$, but it has a disadvantageous influence on the measurement accuracy of the light intensity distribution $I_F(r)$ in the part of the image in which the diffraction rings appear. The maximal light intensity in those rings is very small compared to the intensity $I_{F\max} = I_F(0)$, Fig. 1, in the central part of the image (first bright fringe $- 0.017 I_{F\max}$, second fringe $- 0.004 I_{F\max}$). The elimination (compensation) of the photocurrent coming from the light background is realized by changing the polarization voltage of the difference amplifier.

The corrected photoelectric current is transduced in the converter system I/U of conversion coefficient $k = 10^5$. With such an amplification the voltage U_w at the output of this system will not exceed 2 V for the useful part of the light intensity distribution I_m (Fig. 1), while for $I_{0\max}$ (in the focus region) the voltage is several times higher. In order to exploit completely the resolving power of the $X-Y$ register (or A/C transdduce)r to mapp the light intensity distribution within the range $I(r) \leqslant I_m$ the appearing voltage pulse must be reduced when the entrance dia-

phragm is positioned in the central part of the diffraction image. This is made in the transistor limiter system in which the level of limitation is selected with the help of a potentiometer.

An increase of the spatial resolving power in the process of scanning the diffraction by applying less and less diameter of the entrance diaphragm D_a (Fig. 2) causes simultaneously some worsening of the signal-to-noise ratio. In the measuring system presented a series of solutions has been proposed which allow us to restrict significantly the influence of the noisy phenomena on the useful transduced signal.

The construction of housings of the photodetector, amplifier, and the systems of transducer and automatic battery supplier allow us to locate them all inside the sleeve (7), Fig. 3. The sleeves (7) and (8) with the interference filter constitute a closed shield playing additionally a part of a screen diminishing the level of the perturbances induced by external electric and magnetic fields.

The measuring system described is an element of the scanning system, designed in order to record the diffraction images appearing during examination of the pulverized liquid stream. It can be exploited in two variants with regulation of x, y distances (Fig. 2) and in the "microscopic" version with additional distance tube. In the first variant a fluent control of the image magnification p is possible, in the other one the magnification is constant and its value corresponds to the transversal magnification of the objective $p = \beta_{ob}$.

The basic property of the measuring system desribed is the possibility of detecting light radiation from an arbitrary small surface. This is especially advantageous when there is a necessity of recording the distribution $I(r)$ characterized by significant spatial diversification of the light intensity. High resolving power and identical sensibility (independent of the detector position along the sccaning line) allow us to obtain data about the light intensity distribution $I(r)$ which can be treated as standard data with respect to the other image recording techniques.

3. Measuring stand

3.1. Stationary measuring stand with direct measurement of the light intensity distribution $I(r)$

In Figure 6, the measuring stand in the basic (stationary) version is shown. Due to the possibility of exchanging the recording system for light intensity distribution $I(r)$ it could be adjusted to realization of different variants of the diffraction method. Because of its significant size, great mass and large number of auxiliary devices the stand is practically connected with the room where it has been installed. It was exploited mainly to make the standard and comparative measurements.

The source of coherent light was the helium-neon HNA-188-S (Carl Zeiss Jena) laser of nominal power 50 mW and AO (Ekwant, Zielona Góra, Poland) of 10 mW power. The plane wave of beam diameter $F = 60$ mm was formed with the aid of ZHL UO (PZO, Warsaw) telescope.

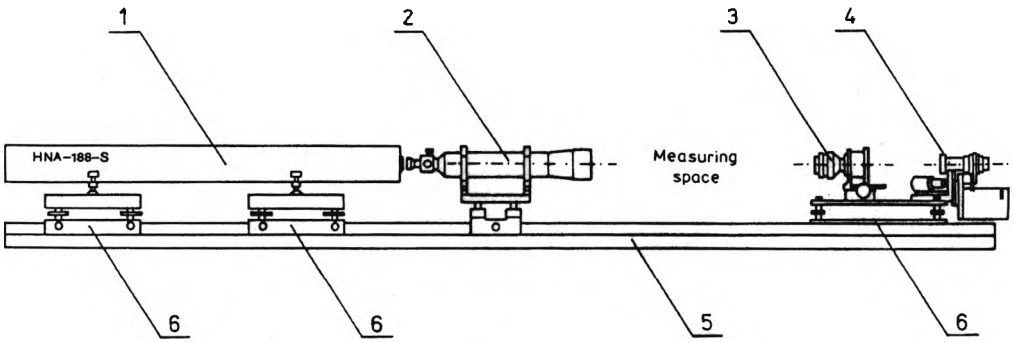

Fig. 6. Measuring stand for recording the diffraction images (1 — gas NHA-188-S laser, 2 — ZHL-UO telescope, 3 — Fourier transforming objective, 4 — scanning and light intensity measuring system, 5 — optical bench, 6 — adjustment stage).

In the measuring system presented in Fig. 7, the recording of the intensity distribution $I(r)$ was done by single scanning of the diffraction image. The position of the objective (1) was controlled preliminarily by the knob (2) and precisely, by the micrometer screw (3). The detection system (8) is mounted on the SK-14 microscope stage rendering the shift in two directions possible. In order to shift the stage in the horizontal plane an electric driver (5) was designed. It consists of a shunt D-5TR motor of 36 W power supplied by direct current of 24 V and a two-step worm gear and a gear transmission.

The transfer of steering signal to the X-Y register (or the analog digital transducer) was realized with the aid of rotary wire resistor located in the housing (7) and coupled mechanically with the motion of the SK-14 stage.

The position of the vertical scanning line can be regulated with the accuracy $\Delta Y = 0.1$ mm in the range $Y_k - Y_p = 50$ mm.

The mesurement space is understood as the region in which the plane wave propagates and thus all the particles of sizes ($10^{-6} - 10^{-4}$ m) included in the light beam between the ZHL UO telescope and the objective performing the Fourier transformation produce their own diffraction images in the focal plane of the objective. An essential problem connected with the accuracy of the results is the adjustment of the length of this space. It should be gradually diminished to such a value for which the drops of the liquid from the stream examined will not be allowed to attain the surfaces of the optical elements.

The aerosol stream entering the measurement space should be formed in a way satisfying the assumptions of the accepted model of diffraction. This means, in practice, the necessity of mechanical restriction of the pulverisation cone with the diaphragms diminishing the number of drops causing the light diffraction.

The scanning of the diffraction image $I(r)$ with a detecting system, which renders possible an accurate measurement of the "diffraction" part of the light intensity distribution $I_F(r)$ and simultaneously does not suffer from destruction when passing through the focus region, allows us to obtain the most complete information about the diffraction of light by the drops of the aerosol examined. This is because it is pos-

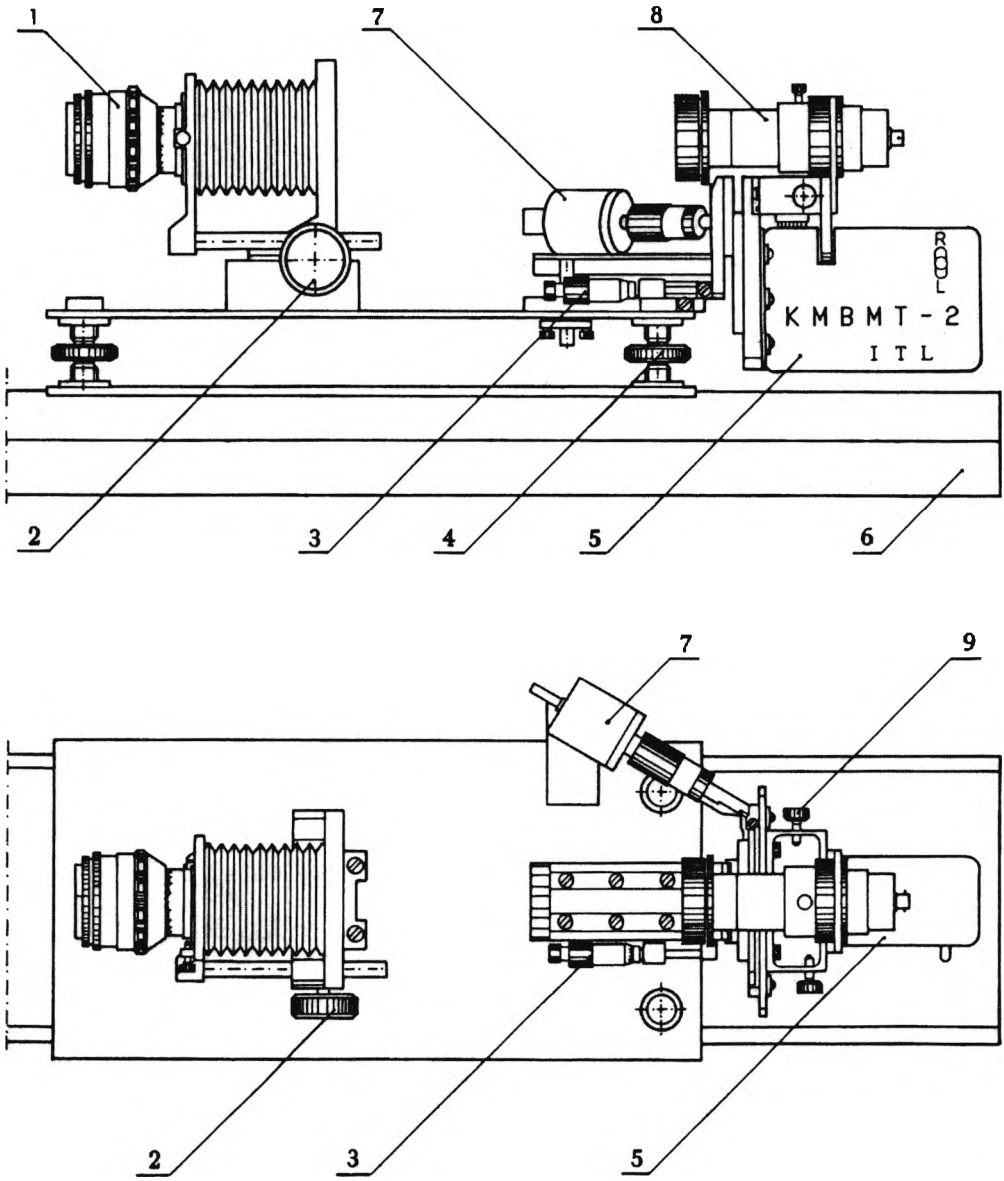

Fig. 7. Scanning and light intensity measuring system for diffraction images (1 — Fourier transforming objective, 2 — hand wheel for preliminary adjustment of the objective position, 3 — micrometer screw for fine adjustment, 4 — vertical adjustment screw, 5 — driving set for SK-14 stage, 6 — optical bench, 7 — housing of the wire resistor, 8 — detection system, 9 — screw limiting the shift of SK-14 stage).

sible to record the diffraction background together with the focus image $I_0(r)$, Fig. 1, before the proper measurements are made, and to determine in this way the corrected distribution $I_F(r) = I(r) - I_0(r)$. The measurement duration of a few seconds

narrows the application range of the scanner to investigation of the stream of pulverized liquid under the stationary condition.

3.2. Stand to measure the average drop diameter for fuel aerosol produced by injectors of turbine aircraft engines

In Figure 8, the measuring stand designed for determining the average diameter of the aerosol drops of fuel produced by injectors of the turbine aircraft engines is

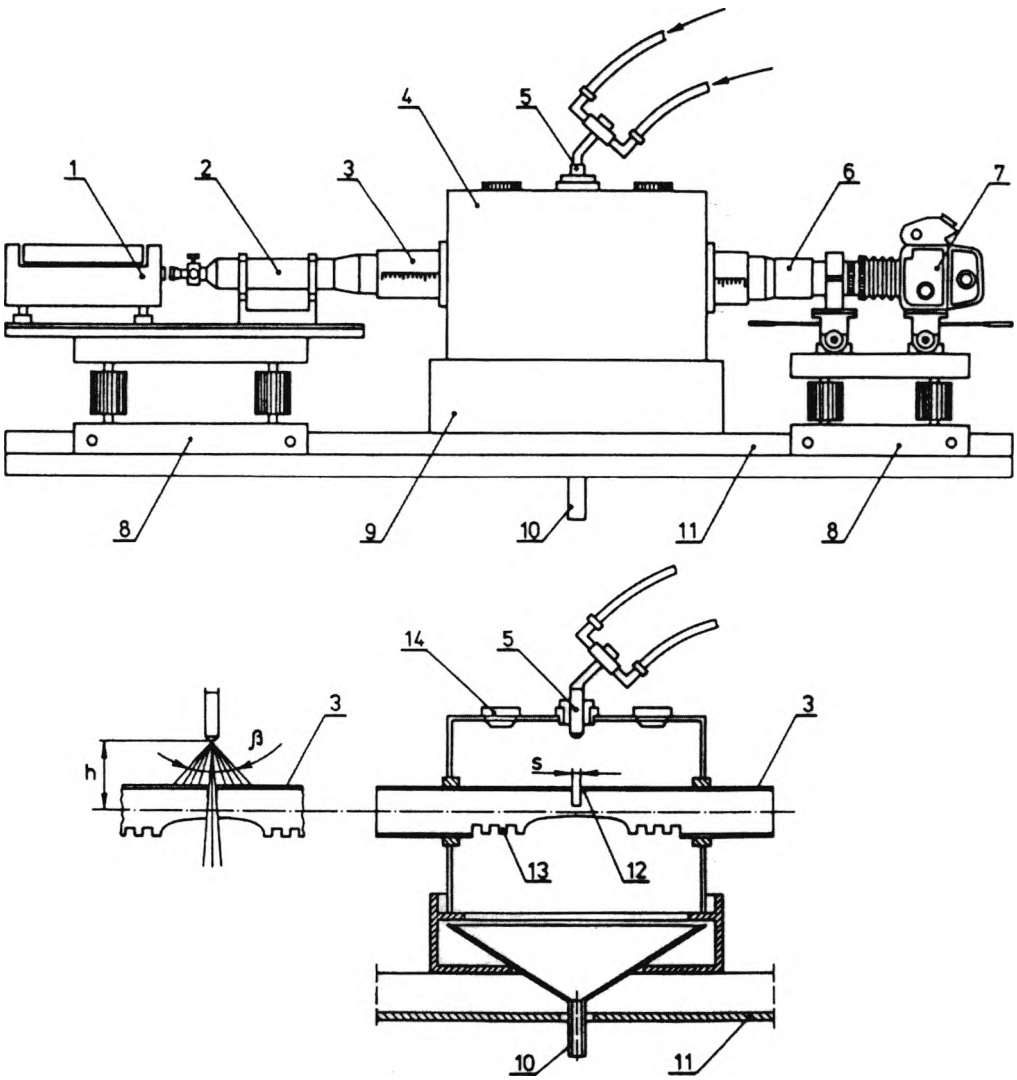

Fig. 8. Stand for measuring the drop sizes in the fuel aerosol stream produced by diagnosed injector (1 — helium-neon AO laser, 2 — ZHL-UO telescope, 3 — shielding tube, 4 — measuring chamber, 5 — injector under test, 6 — MC VOLNA-3 objective, 7 — KIEV 88 TTL (60 × 60) photographic camera, 8 — assembling stage, 9 — gutter for the fuel run-off, 10 — run-off conduit for fuel, 11 — optical bench, 12 — entrance hole in shielding tube, 13 — run-off holes, 14 — plug for ventilation holes).

presented. The plane monochromatic wave was obtained by transforming suitably the He-Ne laser beam with the aid of ZHL UO telescope. The Fourier transforming of the light wave passing through the measurement space was performed by the MC VOLNA-3 objective of focal distance $f = 250$ mm. For photographic recording the ZENIT-12 × P and KIEV 88 TTL cameras were employed. The optical measurement system in the version presented in Figs. 6 and 7 can be used only to examine the starting injectors of small fuel discharge ($Q = 4-10$ l/h).

The main injectors of turbine aeroplane engines are of much higher fuel delivery ($Q = 20-600$ l/h) which causes too large a number of fuel drops in the space "transilluminated" by the plane monochromatic wave. This space must be limited to the degree justifying assumptions of the accepted diffraction model. In the upper part of the enlarged measurement chamber (10) there exist a hole which, after having applied the proper reduction tube, renders it possible to install the injectors of various types.

The element restricting the number of drops in the measurement space has the form of a protecting tube (3) with a transversal hole of width $s = 20$ mm. The distance between the injector output and the tube axis (the latter identical with the axis of the optical system) is $h = 250$ mm. One end of the tube is slid over ZHL UO telescope while the other over the MC VOLNA-3 objective. In this way the tube (together with the measurement chamber) plays an additional role of optical shield, rendering it possible to carry out the measurements in illuminated rooms without the necessity of applying interference filters. In the upper part of the measuring chamber (10) there are four ventillation holes which are closed with plugs (14) during the measurements. The proper positioning of all the elements of the measuring system is possible thanks to two mounting stages (7) of controlled height, fastened to the rigid optical bench (11).

4. Measurement of the average drop diameter of fuel aerosol

4.1. Dependence of substitution diameter D_z on the measurement duration

The basic feature of the fuel stream, sprayed to the closed chamber inside, is its diversification both in time and space. This is true for both the number of the fuel drops in the unit volume and their sizes.

The results of a series of preliminary measurements made over constant time intervals indicated decreasing values of the substitution diameters $D_z = D_{10}$. This was caused by the appearance of the high number of drops in the region of measuring beam coming from the outside of the pulverization cone (the so-called secondary drops), the sizes of which suffered from diminishing due to evaporation, collisions with other drops or with the walls of the measurement chamber.

The introduction of the shielding tube (3, in Fig. 8) restricts the access of the secondary drops to the space through which the plane monochromatic wave propagates. However, the effectiveness of the shield operation decreases with time since the secondary drops diffuss to the shielding tube inside by the efflux holes (13, in Fig. 8).

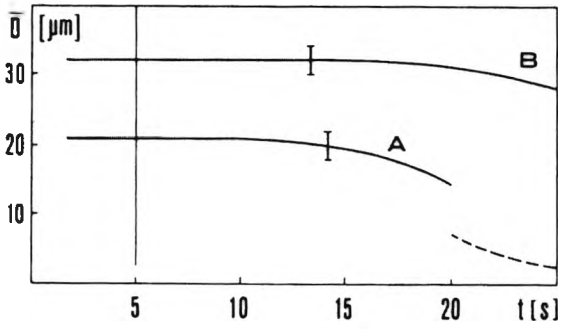

Fig. 9. Substitution diameter $D_z = \bar{D}(t)$ of the drops of fuel aerosol stream in the measurement space restricted by the shielding tube slit as dependent on the measurement time (A – main injector of K 108-012 type, fuel pressure $p = 4.5$ MPa, B – starting injector of K 108-767 type, fuel pressure $p = 0.5$ MPa, width of the measuring slit $s = 20$ mm, shielding tube diameter $D = 110$ mm).

In Figure 9, the results of measurement of the average drop diameter $\bar{D}(t)$ in the pulverization cone for the main injector (curve A) and starting injector (curve B) of the Lis-5 engine are presented. In the case of the main injector of K 108-012 type the value $\bar{D}(t)$ is constant (within the limits of measurement error) during about 10 s from the time the injector has been actuated. The diffusion of the secondary drops to the inside of the shielding tube causes a reduction of the average value of the drop diameter $\bar{D}(t)$ for the working time on the injector $t > 10$ s. After 20 s of the pulverization of the fuel into the inside of the measurement chamber the value of the drop diameter $\bar{D}$ diminishes by about 30%.

The switching off of the injector does not cause the immediate disappearance of the diffraction image. Instead, its diameter increases considerably while its intensity decreases. The complete decay occurs first after several minutes when the fuel drops existing in the measurement space evaporate totally. The intensity of the phenomena described is the highest for the injectors of great delivery of the fuel $Q(t)$. The diffusion of the secondary drops can be delayed, increasing the space to which the pulverized fuel stream is introduced.

4.2. Dependence of the substitution diameter $D_z(h)$ on the distance of the injector nozzle

The choice of the distance h between the optical axis of the measuring line and the injector nozzle (Fig. 8) was preceded by observation of the pulverized fuel stream and the preliminary measurements. For all the injectors examined three zones could be distinguished: zone of compact stream, zone of decay and zone of drops. The light intensity distributions $I(r)$ appearing in the decay zone of the stream are of ellipsoidal symmetry. In the drop zone the diffraction images were circular and their dimensions increased with of the distance h from the diffuser nozzle.

In Figure 10, the results of measurement of the average drop diameter in the pulverization cone of the starting injector of K 108-767 type (for the fuel forcing pressure $p = 1$ MPa and the light beam diameter $D_f = 10$ mm) at different distances h from the nozzle output are presented.

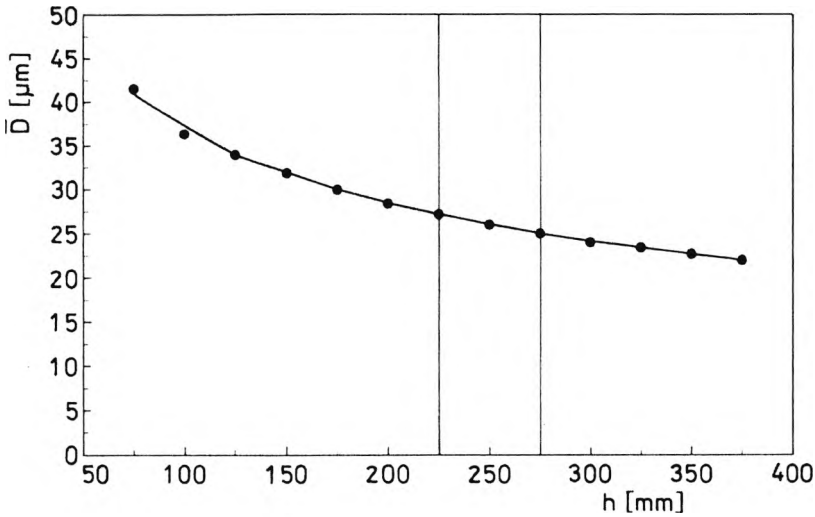

Fig. 10. Average diameter $\bar{D}$ of the drops in the pulverization cone produced by the starting injector of K 108-767 type as dependent on the distance h between the exit nozzle and the axis of the optical measurement line (fuel pressure $p = 1$ MPa).

The character of the dependence $\bar{D} = D(h)$ was the same for all the types of the pulverizing devices examined. The values of the optical parameters of the measuring line $h = 250$ mm and $D_f = 50$ mm have been accepted as being constant for the injectors since then the measurement space was always in the zone of drops.

4.3. Restriction on the drop number in the measurement space

The introductory measurements proved that there is a necessity of restricting the number of drops in the space through which the plane wave propagates. The number of drops which can attain directly this space depends on the fuel discharge $Q(p)$, the width s of the entrance slit (12, in Fig. 8) and the distance h at which the axis of the shielding tube (3, in Fig. 8) is positioned. The slit width $s = 20$ mm was chosen (for $h = 250$ mm) so that for the injector of 37.03.95 type (of highest fuel discharge $Q(p)$) the assumptions of the diffraction model be satisfied.

Because of the sizes of the MC VOLNA-3 objective (exit lens diameter $D_f = 75$ mm) the diameter of the beam illuminating the drop stream was limited to the value $D_f = 50$ mm. Therefore, the measurement space (1) shown in Fig. 11 forms a quasi -cylinder of volume ~ 40 cm^3. In order not to limit the measurements of drop sizes to the middle of the pulverized stream of the fuel the shielding tube was shifted in the extreme (3, 3′) and intermediate (2, 2′) positions.

The distance p, by which the entrance slit should be shifted, was determined on the basis of the value of the angle β of the pulverization cone

$$p = \left[(2h - D_t) \tan\left(\frac{\beta}{2}\right) - s \right]. \tag{7}$$

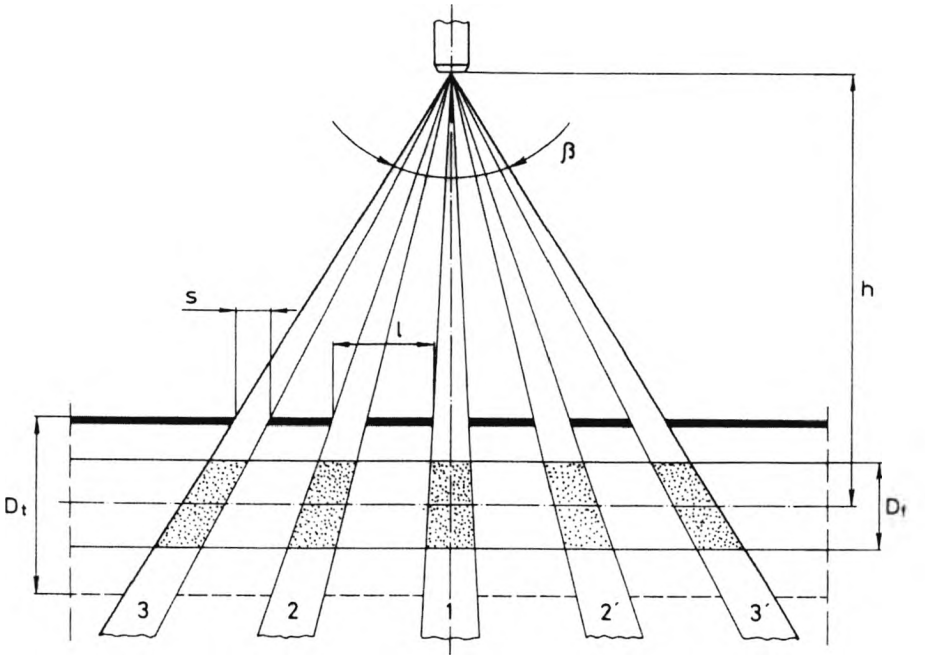

Fig. 11. Shape and position of the measurement space, *i.e.*, the volume of the pulverized fuel stream separated by the entrance slit and illuminated by a plane monochromatic wave (3, 2, 1, 2′, 3′ – consecutive positions of the shielding tube).

After having done many trials it has been found that the drop size $\bar{D} = (D_3 + D_2 + D_1 + D_{2'} + D_{3'})/5$ calculated as an average value from the measurements in the five regions (3, 2, 1, 2′, 3′) is (within the accuracy of the method) consistent with the value obtained from the measurement series in which the distance p of the tube shifting was equal to the width s of the entrance slit.

4.4. Substitution drop diameter D_z for the fuel injectors of turbine aircraft engines

The measurement of the substitution diameter D_z of the drops for different types of injectors of turbine aircraft engines were performed according to a rigorously defined procedure. The diffraction images were recorded after 5 s from the moment of injector activation (Fig. 8). After making a photo the injection of the fuel to the inside of the measuring chamber (10) was stopped. From the four holes positioned in the upper part of this chamber the plugs (14) were removed in order to accelerate the process of drop evaporation. After 20–30 min the ventilation holes were closed again and the image of the diffraction background was recorded prior to the proper measurement.

The suitability of the injectors prepared to measurements of the substitution diameter D_z of the drops was verified on corresponding diagnostic stands (of W-1761, W-1762, Ka-S/W and URS-97-R types), [8]. The PSM-2 fuel of temperature 293 $\pm$1 K was used.

Table 3. Average drops diameter $\bar{D}$ of starting injector of the K 108-767 type of Lis-5 engine.

Starting injector of K 108-767 type of Lis-5 engine		
Injector delivery $Q(p)$	0.15 MPa	4.2–4.8 l/h
	0.60 MPa	8.3–9.3 l/h
Angle of the pulverization cone $\beta(p)$	0.15 MPa	55°–75°
	0.60 MPa	55°–75°
Pressure for leak tightness test	5 MPa	
Average drop diameter $\bar{D}$	0.50 MPa	32±2 μm
	1.00 MPa	26±2 μm

The results of measurements for four types of injectors and the conclusions from the examinations were reported in papers [8], [17] and [18]. For the sake of exemplification the average diameter of the drops $D_{\bar{z}}$ is shown in Tab. 3, for a starting injector of K 108-767 type applied in turbine jet engine of "Lis" series. Its construction is illustrated in Fig. 12. In a cylindric swirler (6) there are two skew holes tangent to its surface. The cone cutting off valve (5) is being opened by an electromagnet. The purification of fuel is done in a slit filter (3).

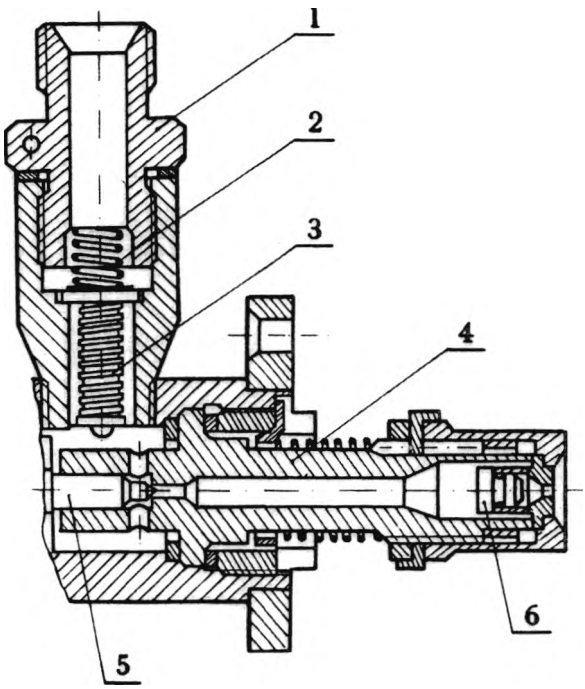

Fig. 12. Starting injector of the K 108-767 type (1 – pipe running off the fuel, 2 – spring, 3 – slit filter, 4 – swirler tube, 5 – fuel cutting off valve, 6 – swirler).

The random error of the substitution diameter D_z determination is included in the range 5 – 10%.

4.5. Summary and conclusions

The results obtained confirmed the possibility of measuring the substitution diameter D_z of fuel aerosol drops produced by the injector of turbine aeroplane engine. The error, if the diffraction method is applied, is contained within the range 5 – 10%.

The insertion of the shielding tube (3), Fig 8, changes the aerodynamic conditions of the fuel stream, which can be a source of the systematic error in the limits 3 – 5%. This estimation follows from the measurements made for starting injectors of both 73.10.9 (engines from the SO series) and K 108-767 types. The results obtained from the measurements with shielding tube (in five zones of the pulverization cone – Fig. 11) and without it were compared with each other. The fuel discharge $Q(p)$ of these injectors did not exceed 10 l/h and the applicability criterion of the diffraction method was satisfied when transilluminating the whole pulverization cone with laser beam.

The necessity of limiting the number of drops in the space of light wave propagation makes the measuring procedure slightly more complex. However, the measurements in a few zones of the stream create the possibility of estimating radial nonuniformity $I(r)$ of the combustion process. The light intensity within the region close to the diffraction image centre is proportional to the number of aerosol drops which were present in the light beam.

The most important shortcoming of the measuring technique described is the diffusion of the secondary drops to the inside of the shielding tube. After having activated some of the main injectors its inside was filled with the evaporating fuel drops already after several tens of seconds which started to be deposited on the surfaces of optical elements. The applied procedure of diffraction image recording allowed us to restrict in an efficient way the influence of the effects mentioned above on the measurement conditions. It is, however, very time-consuming and for this reason difficult to apply for routine diagnostic examinations.

The effect of diffusion of secondary drops into the region of optical "measurement line" can be minimized by pulverizing the fuel to the free space. After having made some trials on the measuring stand shown in Fig. 13 it could be stated that the time between the consecutive measurements can be shortened to about five minutes.

The improved diffractive image recording when injecting the fuel into free space can be achieved in the darkened rooms or after placing an interference filter in front of the photographic camera objective. The application of the filter facilitates significantly the measurement but simultaneously raises the level of diffraction background. The lowest level of this background was attained when between the objective forming the plane wave and the objective Fourier transforming the light beam passing through the aerosol stream there were no additional optical elements (diaphragms, shielding windows, filters and the like). The distance between these objectives should be possibly small since the light diffraction is caused both by drops

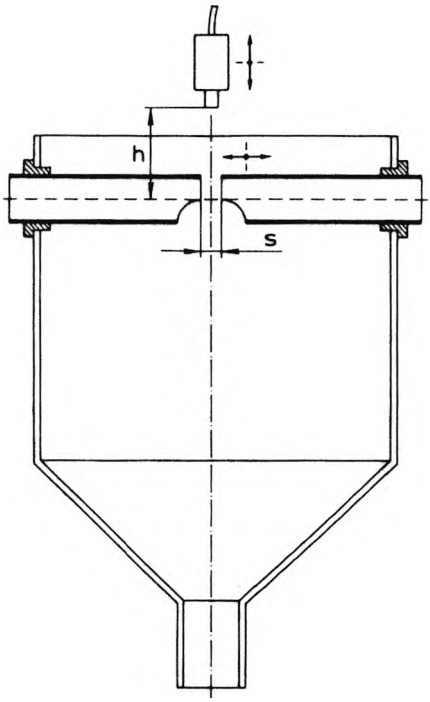

Fig. 13. Scheme of the testing stand with opened measuring dome.

of the pulverized fuel and the particles of the water vapour and all kinds of pollutants suspended steadily in the air.

The application of the measuring procedure described earlier consisting in pulverizing the fuel only during a few seconds with half-hour breaks between the recording of consecutive photos rendered it possible to diminish the distance between the edge of the pulverization cone and the surfaces of the objectives to ~ 1 m.

The diffraction method of determining the substitution diameter $D_z = D_{10}$ of the drops can be particularly useful when making serial comparative measurements for injectors of the same type.

5. Verification of diffraction measurement methods

All the variants of the diffraction method presented are based on the same model of electromagnetic wave – dispersion medium interaction. Thus, the average size of the elements causing diffraction of the light wave should be (within the error limits) the same, independent of the processing procedure applied to the experimental data.

Verification of the coherence of the particular variants of the diffraction methods is relatively simple in the case of monodispersive media. Then, the results obtained by analysing the various fragments of the light intensity distribution $I(r)$ can be compared with the values calculated on the basis of diffraction ring positions.

It is much more difficult to estimate the measurement accuracy in the case of polydispersive media, which follows mainly from the lack of objects which could be taken as suitable standards. The measurement error was determined by comparing the sizes of the standard elements with those obtained from the analysis of their diffraction images (waveguide fibers, glass spheres). Also, some masks produced by photographic techniques with a set of spots the diameters of which created typical statistical distributions $\rho(D)$ of precisely defined parameters (D_z and $d = \sigma/D_z$) were used. In the process of calibration some biological preparations in the form of discs of diameter ~ 7.5 μm and thickness ~ 2 μm appeared to be convenient due to the possibility of direct measurement of diameters with the help of optical microscope.

In the course of control measurements the coherence of all the variants of diffraction method was confirmed. The highest accuracy is achieved when applying the linear transformation of the light intensity distribution $I(r)$, [10]. The approximation of the quasi-linear fragment of the relation $I(r)$ (of direct or photographic recording of the diffraction image) and exploiting the characteristic point $I_{0.57}$ produce results charged with greater error.

A complete analysis of the average diameter D_z of the aerosol drops can be carried out after taking account of the influence of the mechanical restriction of the number of aerosol drops which can reach the optical measurement line. The application of the shielding tube with calibrated slits (Figs. 8 and 11) is one of the ways of separating the chosen zone of the pulverization cone. This is ingeration, however, into the process of liquid stream decay which deforms the object examined to the degree difficult to estimate. Such an operation appears to be necesary in order to create the conditions allowing the assumption of single-scattering model of light wave diffraction. An alternative solution would consist in taking account of multiple-scattering of the light beam which is a much more complex problem [19], [20].

References

[1] MROCZKA J., *Metrological problems of scattered light application for particle size distribution investigation in dispersed solutions*, Metrologia i Systemy Pomiarowe (in Polish), No. 4, Warszawa 1990.

[2] BAUER D.,. IVANOFF A., C. R. Acad. Sci., Paris **260** (1965), 631.

[3] BAYVEL L.P., JANES A.R., *Electromagnetic Scattering and its Applications*, Appl. Sci. Publ., London 1981.

[4] DUNTLEY S.Q., J. Opt. Soc. Am. **53** (1963), 214.

[5] KULLENBERG G., Deep Sea Res. **15** (1968), 423.

[6] MULY E.C., FROCK H.N., Opt. Eng. **19** (1980), 861.

[7] JANKOWSKA-KUCHTA E., *Diffraction methods of the burners fuel atomization quality assessment* Silniki Spalinowe, No. 2–3 (1986), 65 (in Polish).

[8] OPARA T., *Metrology Aspects of Phenomena Investigation Arising in the Turbojets Burners Spraying Cone* (in Polish), WAT, Warszawa 1996.

[9] OPARA T., Biul. WAT (in Polish) 43 (1994), 135.

[10] OPARA T., *ibidem*, p. 147.

[11] OPARA T., *ibidem*, p. 155.
[12] OPARA T., WDOWIAK S., Biul. WAT (in Polish), **41** (1992), 61.
[13] OPARA T., Biul. WAT (in Polish) **42** (1993), 129.
[14] MEYER-ARENDT J.R., *Introduction to Optics* (in Polish), PWN, Warszawa 1977.
[15] BORN M., WOLF E., *Principles of Optics*, McMillan Co., New York 1964.
[16] PLUTA M., *Advanced Light Microscopy*, Vol. I (*Principles and Basic Properties*), Vol. II (*Specialised Methods*), Vol. III (*Measuring Techniques*), PWN, Warszawa 1988–1989–1993.
[17] OPARA T., Biul WAT (in Polish), **41** (1992), 91.
[18] OPARA T., J. Thermal Sci. **6** (1997), 298.
[19] CZERWIŃSKI M., MROCZKA J., REN K.F., GRÉHAN G., GOUSBET G., *Scattered Light Predictions Under Multiple Scattering Conditions with Application to Inversion Scheme*, [In] Proc. 7-th European Symposium *Particle Characterization*, Nürnberg, March 10–12, 1998.
[20] CZERWIŃSKI M., MROCZKA J., WYSOCZAŃSKI D., *Inverse Problem in Multiple Light Scattering – Hybrid Method Application*, [In] Proc. MUSCLE 10, Tenth International Workshop on Multiple Scattering Lidar Experiments, Florence, April 19–22, 1999.

Received January 10, 2000
in revised version July 20, 2000